



# A novel measurement strategy and a dedicated sampling cell for the parallel characterization of organic and inorganic constituents in polymer samples by concurrent laser ablation ICP-OES and EI-MS

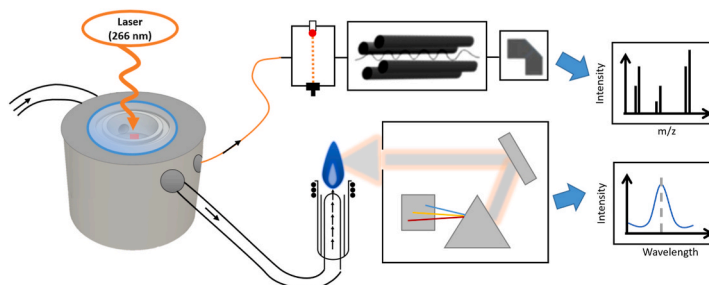
Laura Kronlachner<sup>\*</sup>, Johannes Frank, Erwin Rosenberg, Andreas Limbeck<sup>\*\*</sup>

TU Wien, Institute of Chemical Technologies and Analytics, Getreidemarkt 9/164, 1060, Vienna, Austria

## HIGHLIGHTS

- New ablation cell design allows direct coupling of laser ablation with EI-MS and ICP-OES.
- EI-MS data allows identification of polymers even in mixture.
- ICP-OES data is vital for detection of additives and impurities.
- Method enables classification and differentiation of polymeric composite material.

## GRAPHICAL ABSTRACT



## ABSTRACT

Polymeric composite materials are gaining importance due to their universal applicability and easy adaptability for their intended use. For the comprehensive characterization of these materials, the concurrent determination of the organic and the elemental constituents is necessary, which cannot be provided by classical analysis methods.

In this work, we present a novel approach for advanced polymer analysis. The proposed approach is based on firing a focused laser beam onto a solid sample placed in an ablation cell. The generated gaseous and particular ablation products are measured online parallelly by EI-MS and ICP-OES. This bimodal approach allows direct characterization of the main organic and inorganic constituents of solid polymer samples.

The LA-EI-MS data showed excellent agreement with the literature EI-MS data allowing not only the identification of pure polymers but also of copolymers, as demonstrated with acrylonitrile butadiene styrene (ABS) as the sample. The concurrent collection of ICP-OES elemental data is vital for classification, provenance determination, or authentication studies. The applicability of the proposed procedure has been demonstrated by analysis of various polymer samples from everyday use.

## 1. Introduction

Polymeric composites are a novel class of materials widely used in many different fields of application. Typical uses include industrial

purposes in the form of raw materials, paints, varnishes, and areas of daily life where they find applications, e.g., as foils and packaging materials. Polymeric composites consist of organic polymer materials with various organic and inorganic additives such as pigments, antioxidants

<sup>\*</sup> Corresponding author.

<sup>\*\*</sup> Corresponding author.

E-mail addresses: [laura.kronlachner@tuwien.ac.at](mailto:laura.kronlachner@tuwien.ac.at) (L. Kronlachner), [andreas.limbeck@tuwien.ac.at](mailto:andreas.limbeck@tuwien.ac.at) (A. Limbeck).

<https://doi.org/10.1016/j.aca.2023.341305>

Received 7 November 2022; Received in revised form 27 April 2023; Accepted 28 April 2023

Available online 29 April 2023

0003-2670/© 2023 The Authors. Published by Elsevier B.V. This is an open access article under the CC BY license (<http://creativecommons.org/licenses/by/4.0/>).

and flame retardants by which the polymeric composite compounds are customized for individual applications [1–3]. Consequently, polymeric composite materials show excellent adaptability and versatility for an abundance of purposes, as their physical and chemical properties can be tuned over a wide range. The increasing reliance on polymeric composite materials requires a reliable and detailed analysis of the quality and composition of the substances in use – in particular, the prevailing type of polymer and the inorganic constituents.

When analyzing polymeric components, the primary information of interest is the composition of the materials [2,4], including the type of polymer, potential additives and contaminants [5,6]. Knowledge about the composition of both the organic and inorganic constituent levels is required for a comprehensive characterization. Questions and issues like these arise in several fields, including plastics processing [7,8], plastics recycling [9–11] and forensic analysis [12–15]. For these purposes, the analysis of polymeric composite materials needs to make the comparison, classification, identification, and assessment of the various compounds possible.

Conventional methods for the determination of chemical structures include techniques that require a preceding sample pretreatment, such as liquid chromatography-mass spectrometry (LC-MS) [5,16,17] and gas chromatography-mass spectrometry (GC-MS) [18,19]. Methods for the direct analysis of the solid polymers include Fourier transform infrared spectroscopy (FTIR) and Raman spectroscopy [20–22], matrix-assisted laser desorption/ionization mass spectrometry (MALDI-MS) [23–25] and pyrolysis gas chromatography-mass spectrometry (Py-GC-MS) [6, 26,27]. Each of the above-mentioned analytical methods has its individual strengths and weaknesses. These range from tedious sample preparation in combination with the ability to separate individual constituents to direct analysis without error-prone sample pretreatment with difficulties characterizing complex chemical structural composition.

Samples like copolymers consisting of several different kinds of monomeric building blocks or mixtures of polymers present a more challenging analytical problem as many methods struggle to characterize and classify them straightforwardly [24,28]. In another distinctive feature, several of the techniques only allow bulk analysis, while others are sensitive to the sample's surface. Depending on the method of choice, the analysis of a polymeric sample results in information on its chemical structure, molecular weight and composition. However, all of the described conventional polymer analysis techniques only provide information on the organic moiety of the sample and do not provide any information on the inorganic constituents of the sample.

Standard methods for elemental analysis applied in material chemistry include X-ray-based techniques, such as X-ray fluorescence (XRF), energy-dispersive X-ray spectroscopy (EDX), or mass spectrometric methods, such as glow discharge mass spectrometry (GDMS) and secondary ion mass spectrometry (SIMS). Although well-established for the analysis of inorganic samples, the investigation of polymers is not straightforward and often impossible with these techniques.

Consequently, comprehensive characterization of composite materials is currently not possible with a single technique. A multimodal approach is required, combining molecular information about the polymer sample with information on the elemental composition. Moreover, for many analytical problems, bulk information is insufficient to provide a satisfactory answer. Thus, spatially resolved measurements are necessary to gain information about possible variations in the composition within the sample (e.g., homogeneous distribution of additives). In addition, direct solid sampling is attractive as it requires little to no sample preparation.

These requirements could be met using laser ablation in combination with suitable detection methods. In the field of elemental analysis, LA-ICP-MS and LA-ICP-OES are both well-known and established methods. Since this approach enables the analysis of non-conductive samples, the technique has become very popular in the analysis of both biological and synthetic polymers in the last years. Applications

range from typical bulk measurements [29] to spatially resolved investigations [30].

Although less common in literature, also the combination of laser ablation with organic mass spectrometry is reported, and studies on the interaction of an ultraviolet laser with organic polymers were already described by Srinivasan and Braren in 1989 [31]. In this approach, the laser system was used for the ablation of finite amounts of sample material. Subsequently, the obtained products were introduced into the MS for molecular analysis. Choi et al. [32], Greenwood et al. [33] and Watanabe et al. [34] report the significant benefits of merging laser ablation, including direct analysis of solid samples, with the capability of qualitative analysis of organic structures facilitated by organic mass spectrometry. However, in contrast to conventional LA-ICP-OES or LA-ICP-MS techniques, the published experimental setups combining laser ablation with organic MS do not allow spatially resolved investigations.

In this work, we describe the development of a novel procedure combining, for the first time, laser ablation with parallel electron ionization mass spectrometry (EI-MS) and ICP-OES detection, enabling concurrent analysis of organic and elemental sample constituents in solid samples. For this purpose, a new ablation cell design was developed, in which the carrier gas flow with the ablated sample material is split into two parts, one for EI-MS analysis and one for ICP-OES detection. The applicability of the proposed LA-EI-MS/ICP-OES procedure was demonstrated by the analysis and classification of polymeric samples based on the information provided by the two complementary analytical techniques on the organic and inorganic sample constituents.

## 2. Experimental

### 2.1. Instrumentation

The ablation of the sample material was carried out using the laser system of a commercially available J200 Tandem LIBS system (Applied Spectra, Inc., Fremont, CA) equipped with a frequency quadrupled Nd:YAG laser (4 ns pulse duration, 266 nm wavelength). The movable XYZ stage of the instrument allowed spatial manipulation of the ablation cell.

A Thermo Scientific DSQ™ II single quadrupole mass spectrometer equipped with electron ionization (EI), as would typically be used in a GC-MS system (Thermo Scientific, Waltham, MA, USA), was used for mass analysis.

A deactivated intermediate polarity fused silica capillary (Supelco, Bellefonte, PA, USA) with an inner diameter of 0.1 mm was used as a transfer line for connecting the ablation chamber to the EI-MS. The capillary was installed using a 15% graphite/85% vespel ferrule (Thermo Scientific, Waltham, MA, USA) and a 1/16 inch lock nut (Swagelok, Solon, OH, USA). The heating of the transfer line was achieved using a CuNi44 resistance wire RD 100/0.6 (0.6 mm diameter, 1.73 Ohm/m, 2.21 A; Block, Verden, Germany) mounted along the capillary within a glass fiber braided insulation sleeving lightly impregnated with silicone (2 mm diameter, Helaglass G6SE; HellermannTyton, Wythenshawe, UK). The temperature was adjusted using a PID control loop controlled by an Arduino® Nano 3.0 (A000005) ATmega328 microcontroller (Arduino, Somerville, MA, USA) and an NTC resistor as the temperature sensor. The power output is controlled by a MOSFET (InfineonHEXFET IRL3705ZPBF; Infineon, Villach, Austria).

A Thermo iCAP 6500 ICP-OES instrument (ThermoFisher Scientific, Bremen, Germany) equipped with an echelle optics and a charge injection device (CID) solid state detector was used to analyze the sample's elemental composition. For connecting the ablation cell with the ICP-OES, PTFE tubing (Deutsch & Neumann, Hennigsdorf, Germany) with an inner diameter of 1 mm and an outer diameter of 3 mm was used.

## 2.2. Design of the ablation cell

Commercially available ablation cells do not allow the desired parallel coupling of laser ablation with two detection techniques since just a single outlet for the carrier gas is available in the cell. Hence, an in-house design for the ablation cell with one outlet for connecting to the EI-MS and one outlet for coupling with the ICP-OES was developed.

A schematic drawing of the cell designed in-house and machined from aluminium is given in Fig. 1. It had a round sample cavity (11 mm diameter, 5.5 mm depth) and two drill holes equipped with push-in fittings (3 mm, M5, Festo, Esslingen, Germany) for the He gas inlet and the exit of the main gas flow, which was connected to the ICP-OES detection unit. At a 30° angle to the main exit, a hole equipped with a septum (12.9 mm Silicona/PTFE, 3.2 mm for GL14, VWR, Radnor, PA, USA) cut to 4 mm diameter was placed, allowing the capillary transfer line to be connected by piercing it through the septum and positioning it above the sample. The septum was fixated using a hollow retaining screw. The cell was sealed using a circular UV-grade fused silica window (20 mm diameter x 1.5 mm thickness) (Crystran Ltd., Poole, UK) to allow transmission of the laser light. It was pressed onto a rubber sealing ring in a milled groove with a specially constructed cell cover and Allen screws to ensure gas tightness.

## 2.3. Chemicals and sample materials

Helium (purity 99.999%) was used as the carrier gas and to purge the cell, and Argon (purity 99.999%) was used for the plasma of the ICP-OES. The gases were obtained from Messer Austria (Gumpoldskirchen, Austria).

Several polymer samples from everyday life applications were collected to demonstrate the method's classification abilities. The polystyrene samples included packaging material (Styrofoam), a CD cover and a serving tray. For the Poly (methyl methacrylate) (PMMA) sample, a plastic microscope slide was used, and the Teflon sample was a raw material used for constructing Teflon sealing parts and for polyacrylonitrile (PAN), technical fibers were used.

For optimization of the measurement parameters of the LA-ICP-OES procedure, the standard reference material NIST 612 (trace elements in glass) (National Institute of Standards and Technology, Gaithersburg, MD) was used.

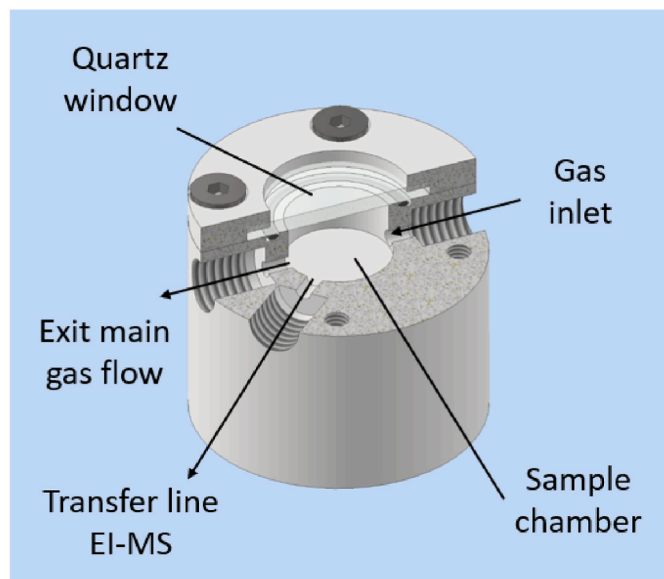


Fig. 1. Construction drawing of the in-house-designed ablation cell for LA/EI-MS/ICP-OES.

## 2.4. Setup of online laser ablation EI-MS/ICP-OES and method development

To analyze a composite material sample, it is put in the ablation cell and sealed tightly using the cell's cover including the fused silica glass. The cell is placed on the XYZ stage of the laser ablation device. Helium with a flow rate controlled by the internal MFC of the J200 is passed through the gas inlet into the cell. In the ablation chamber, the gas flow is split for concurrent EI-MS and ICP-OES analysis.

Due to the vacuum within the EI-MS ion source and analyzer, there is a constant suction at the open end of the capillary, which is used to transport a minor part of the ablation products to the EI-MS. To overcome potential analyte losses due to condensation of less volatile species, the capillary line is heated to a temperature of 90 °C using the mounted heating jacket. The majority of the He flow leaves the ablation chamber through the gas outlet connecting the cell with the ICP-OES due to the larger diameter of the tubing in comparison to the capillary attached to the EI-MS. The He stream carrying the ablation products is mixed with argon using an in-house-built concentric gas mixer and finally introduced into the plasma of the ICP-OES.

For carrying out measurements, the laser is focused on the sample surface and fired through the quartz glass window covering the ablation cell. Experiments are conducted using single-shot patterns as well as stacked meander line patterns. If not stated otherwise, 100 laser shots with a laser beam diameter of 100 µm, laser energy of 1.0 mJ and a frequency of 10 Hz are used for ablation. A Helium gas flow in the ablation cell of 200 mL/min is applied.

The EI-MS measurements are conducted using positive ion detection mode and ionization energy of 70 eV. Full scan measurements are done between the mass-to-charge ratio ( $m/z$ ) of 45 and 200 with a dwell time of 20 ms. For the evaluation of all EI-MS measurement results, the mass spectra are averaged, background corrected and normalized to the base peak of the resulting spectrum. The ICP-OES measurements are conducted using a plasma power of 1300 W and a radial observation height of 12.0 mm. ICP-OES signals are recorded and processed by Thermo iTEVA software. Signals are monitored for 30 s in "transient signal" mode, and data points are collected every 0.5 s. The signals are integrated and background-corrected.

The make-up Ar gas flow is set to 0.25 L/min, the auxiliary gas flow to 0.8 L/min and the coolant gas flow to 14 L/min. Investigations were focused on elements that are either common additives or typical contaminants in polymeric composite materials. The chosen lines under investigation were: Al (396.1 nm), Ba (455.4 nm), C (247.8 nm), Ca (393.3 nm), Fe (259.9 nm), Mg (279.5 nm), Si (251.6 nm), Sr (407.7 nm) and Ti (334.9 nm). For data evaluation of the ICP-OES results, a ratio of the signal intensity of each of the elements to the intensity of the carbon signal was calculated to achieve normalization to the C-signal.

Fig. 2 schematically illustrates the temporal sequence of the events appearing within the course of a measurement point. This includes the

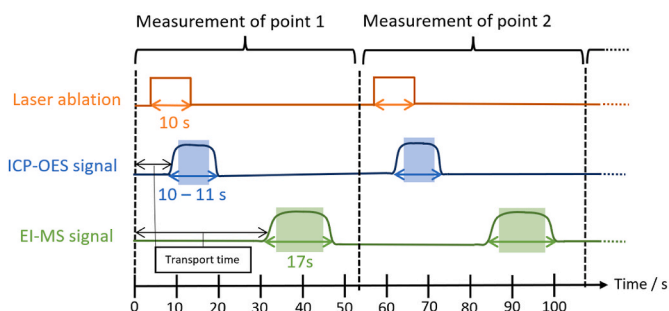


Fig. 2. Schematic diagram of the events during a measurement showing the timing of the laser ablation relative to the ICP-OES and EI-MS signals for the same ablated sample portion as well as their individual transport times and integration windows.

laser ablation event and the formation of the parallel ICP-OES and EI-MS signals which are recorded after a delay corresponding to the individual transport times to the respective detection systems. The blue and green boxes over the ICP-OES and EI-MS signals highlight the plateau shaped sections of the detected signals. These periods of roughly constant signal intensity indicate the continuous detection of ablated sample material. Hence, their starting and end points were used as limits for averaging and integration of the signals.

### 3. Results and discussion

#### 3.1. Cell design and optimization of measurements conditions

Conventional ablation chambers fail to achieve a satisfying online coupling of LA with EI-MS due to the incompatible requirements of a reasonably fast washout of the sample aerosol after the ablation and a low gas flow for the EI-MS to avoid compromising the high vacuum.

While LA requires a higher gas flow of 200–1000 mL/min to purge the ablation cell efficiently, EI-MS is operated under high vacuum conditions, which are impossible to maintain with such a high gas flow. Thus, the gas flow used for sample introduction must be limited to a range of approximately 1 mL/min. Published solutions for that problem rely on separating the laser ablation process and the EI-MS analysis using a trap or a sample loop, allowing sample injection into the EI-MS with a reduced gas flow [32–34]. However, with this approach, only bulk measurements with EI-MS are possible, spatially resolved investigations such as imaging or depth profiling are prevented. Moreover, with this experimental setup, the parallel analysis of the elemental sample composition is not feasible.

To allow the online coupling of the two techniques, the development of an improved ablation cell that allows a severe split of the gas flow was necessary. In the constructed ablation chamber, the total flow of the Helium was divided into the main flow directed to the ICP-OES and the capillary transfer line flow directed to the EI-MS. Since, according to the Hagen-Poiseuille equation, the volumetric flow in tubing mainly depends on its diameter and its length, a capillary with a 0.1 mm inner diameter was chosen to ensure low flow rates. However, besides the carrier gas flow, also other instrumental parameters such as the applied laser energy or length and temperature of the transfer capillary have to be considered, which influence the quality of the subsequent EI-MS and ICP-OES analysis.

Optimization of operational parameters was performed with the goal of improving the sensitivity of the measurements as well as the reproducibility of the data. For the optimization process, the signals yielded from 10 shots within 1 s on a PMMA sample with 0.86 mJ laser energy were compared.

The helium flow rate significantly affected the duration and intensity of the detected EI-MS signals. It was optimized to find a compromise between the washout behavior of the cell and the intensity of the signals ensuring good sensitivity. The flow rate was varied between 100 and 600 mL/min in 100 mL/min steps resulting in an optimum observed at 200 mL/min, where both signal intensity and washout behavior were satisfactory. A lower gas flow resulted in higher signal intensity but poor peak shape indicating bad washout behavior, while a higher flow improved the washout but reduced the signal intensity. In contrast, the helium flow had negligible influence on the ICP-OES signals and only affected the response time delay from the ablation process until the signal was detected.

The length of the transfer capillary influenced the split ratio of the flow rates reaching the EI-MS and the ICP-OES since the flow resistance in the capillary transfer line depends on its length. A shorter length of the capillary increased the gas flow into the MS, resulting in high signal intensities but only moderate reproducibility. With increasing capillary length, the flow is reduced, improving the reproducibility but decreasing the intensity of the signals.

Thus a compromise between signal intensity and reproducibility was

necessary. The capillary length was varied between 0.5 and 5 m in steps of 0.5 m showing an optimum at a capillary length of 2 m for the EI-MS measurement while it did not affect the ICP-OES measurement. The influence length of the PTFE tubes connecting to the ICP-OES was negligible regarding the detected signals and again only affected the response time delay.

The setup was further improved by heating the transfer line to the EI-MS to counteract unwanted retention and thus separation of the different ablation products during their transport through the capillary.

For inorganic sample constituents, the occurrence of retention is rather unlikely during the transport through PTFE tubing. In contrast, this is possible in the case of organic compounds transported within a capillary. Ideally, the laser ablation process would result in one sharp signal for both detection systems. In reality, the EI-MS signal is broadened versus the ICP-OES signal. In extreme cases, the species generated within the same ablation process would be detected in the EI-MS as separated peaks due to their different travel velocity through the capillary transfer line, while the ICP-OES still detects only one single peak at 247.8 nm, which is the wavelength used for carbon detection. Moreover, for species with stronger retention in the transfer line, a distinctly delayed arrival at the detector could be expected. Thus, mixing of the ablation products from subsequent laser shots is possible. In a worst-case scenario, broadening of the signal results in a continuous, low-intensity signal rather than discrete, high-intensity signals resulting from the individual laser pulses.

During parameter optimization experiments, laser ablation of a PMMA sample during 10 s with 10 Hz was monitored. The analysis at room temperature resulted in broad signals with at least two peaks as shown in Fig. 3. The observed width of the EI-MS signal is approximately 44 s, making it more than three times longer than the corresponding ICP-OES signal with a mean duration of 12 s only. This outcome indicates that fragments experience different retention within the capillary. Heating the capillary transfer line to an outer temperature of 90 °C (the maximum temperature achieved with the setup) improved this undesirable effect significantly and resulted in one sharp signal peak with a peak width of 17 s with higher signal intensity and thus higher sensitivity for the same ablation process (Fig. 3).

In the ablation chamber, on the contrary, no condensation was observed, which is due to the high carrier gas flow (200 mL/min) in combination with the small volume of the ablation cell (<0.5 cm<sup>3</sup>). This efficient washout of the sample aerosol out of the cell and prevented notable redeposition and condensation.

After optimization of the transfer of the ablation products to the

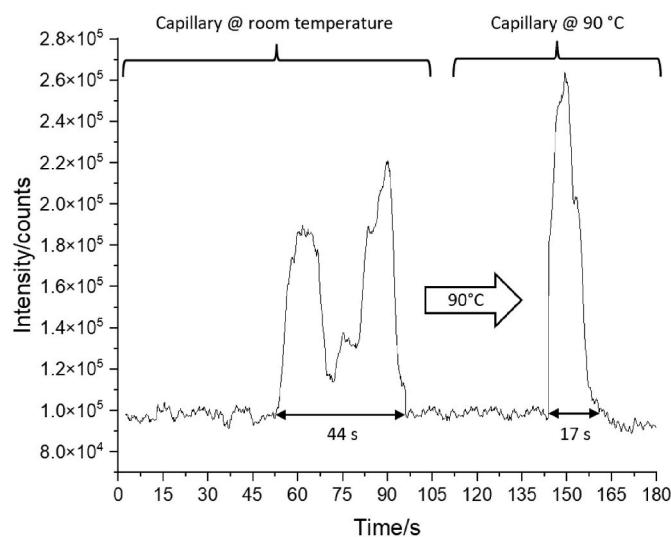


Fig. 3. Comparison of the EI-MS signal width and peak form of 100 laser shots within 10 s on PMMA at room temperature and at 90 °C.

applied detection devices, optimization of the ablation process was also considered necessary. In particular, the influence of laser energy on the subsequent EI-MS and ICP-OES analysis has to be investigated. Using higher laser energy resulted in a higher ablation rate and thus more intense signals overall in both the EI-MS and the ICP-OES measurement.

However, besides sufficient sensitivity, the method also requires an appropriate balance between the desorption of the sample material and the fragmentation of the organic molecules. For the identification of unknown polymers, conventional fragmentation patterns are required to make database comparison possible.

Experiments performed with varying laser energies indicated that the applied conditions affected the abundance of the detected fragments significantly. With lower laser energy, less fragmentation occurred, resulting in the more frequent formation of characteristic fragments with larger  $m/z$  ratios. Vice versa, higher laser energy generally resulted in more fragmentation into smaller fragments.

This observation is illustrated in Fig. 4, which shows the EI-MS spectra detected after ablating bulk PMMA with laser energy of 0.25 mJ and 1.90 mJ, respectively. With lower laser energy, a higher intensity for the fragments with bigger  $m/z$  ratios of 69 and 100 was observed, while lower signals were detected for the  $m/z$  value of 50. Higher laser energy showed the opposite effect. For the ICP-OES detection, the laser energy solely affected the intensity of the measured signals. Increasing the energy from the lowest to the highest setting resulted in four times higher C-signal at the monitored wavelength of 247.8 nm.

A laser fluence of 1.0 mJ turned out to be a good compromise for the investigated polymer samples showing both sufficient signal intensity and structural information for smaller and bigger fragments when performing bulk measurements. With too much fragmentation of the polymer molecules due to high laser energy, the identification of the compounds using spectral libraries/literature data would be significantly hampered.

### 3.2. Differentiation of polymers

Different polymers were measured using the optimized LA-EI-MS/ICP-OES procedure. For classification purposes of the polymeric bulk material, a pattern of 100 shots with a frequency of 10 Hz, a laser beam diameter of 100  $\mu\text{m}$  and a laser energy of 1.0 mJ were applied. A mass range of  $m/z$  45 to 200 was chosen for the EI-MS measurement, and for the ICP-OES analysis, the standard conditions were used.

An average EI-MS spectrum was calculated using the individual obtained spectra measured throughout the signal length. After background subtraction, the intensities were normalized to the base peak of the resulting spectrum.

In a first series of experiments, polyacrylonitrile (PAN), polystyrene (PS), polytetrafluoroethylene (PTFE) and poly (methyl methacrylate)

(PMMA) were measured. The ablation generated steady signals in the EI-MS detection but also for ICP-OES showing a rise within the first seconds, a plateau during the duration of the ablation and a drop after the ablation had ended. As expected, the obtained elemental information allowed no identification of the prevailing polymers, although the signals for the trace elements Ca and Mg normalized to the carbon signal analyzed by ICP-OES showed significant variations (Fig. 5a). These differences in the elemental fingerprints stem from the intentional addition of materials such as pigments, fillers and flame retardants [3] as well as contaminations from the raw materials or processing.

The normalization to the carbon signal is necessary to account for different laser ablation rates and different aerosol particle size and number that may occur with different sample materials. Hence, the simple comparison of measured signal intensities is not straightforward. The normalization to one of the measured elements used as an "internal standard" is necessary to allow meaningful interpretation of the data. In the case of organic polymers, this normalization can be done to the intensity of the carbon signal since it is the main component in all of the samples.

The four different polymers could be easily distinguished using their characteristic organic fragments obtained in the EI-mass spectrum, as shown in Fig. 5b. For the materials under observation, the characteristic fragments of the polymers were in excellent agreement with the literature data of the monomers (as found in Ref. [35]), which allowed simple classification and even identification without complex statistical data analysis.

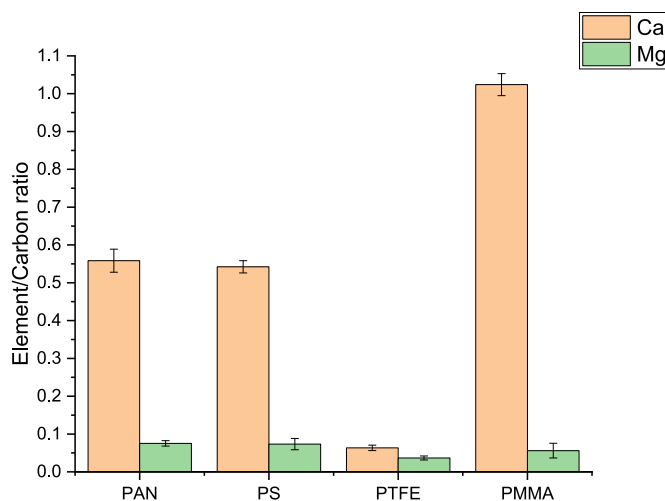


Fig. 5a. Element (Ca and Mg) to carbon-ratio of the four different polymer samples detected with ICP-OES.

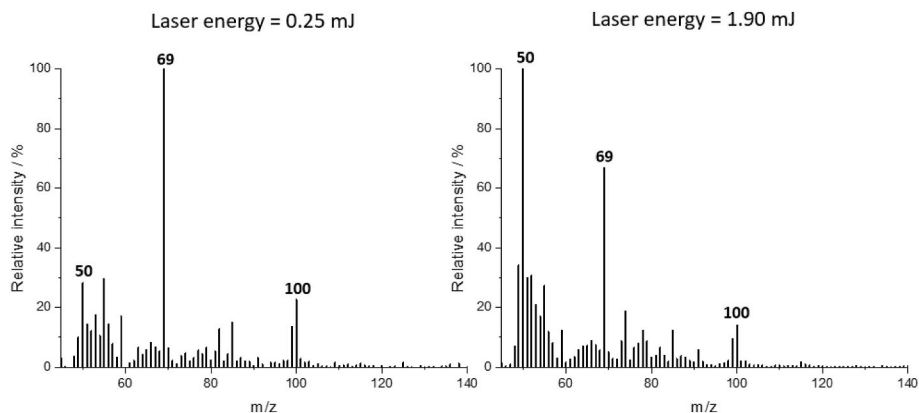


Fig. 4. EI-MS spectra of ablated bulk PMMA with laser energy of 0.25 mJ (left) and 1.90 mJ (right).

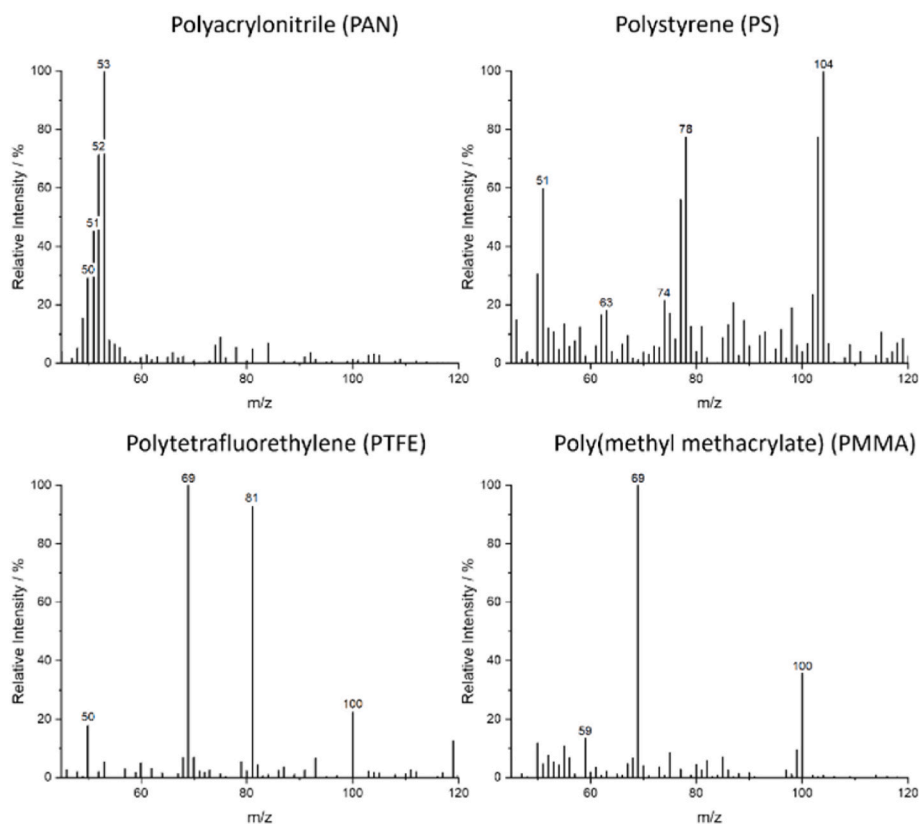


Fig. 5b. Laser Ablation- EI-MS spectra obtained from four different polymers samples.

Table 1 presents the assignment of the most abundant fragment ions detected with different sample material. The direct interpretation of mass/charge ratios and intensity of the different fragment ions, or – in case of availability of dedicated spectral libraries – a library search provides information on the polymer investigated. In combination with basic knowledge about the origin of the polymer sample and the possible areas of applications for common polymers, a specific statement about the identity of the polymers can be made. For further advanced identification, a larger database of EI-MS data of laser-ablated polymer samples needs to be created.

In a second set of experiments, copolymers and composite samples consisting of more than one kind of polymer were investigated. Measuring EI-MS of polymers also gives the vital advantage of quickly identifying the different species of monomers in a mixture or even in copolymers. An Acrylonitrile butadiene styrene (ABS) copolymer sample was investigated using the same measurement conditions as stated above. The mass spectrum of the ABS shows the characteristic fragments of all three monomers and allows characterization of the copolymer with ease, as shown in Fig. 6.

In contrast to the studies reported so far, the proposed procedure allows spatially resolved measurements. This special benefit is accomplished by directly coupling the developed ablation cell with the EI-MS analysis. Thus, spatially resolved information about the occurrence of individual polymers in structured samples can be gained. Applicability has been demonstrated by the analysis of an artificial sample prepared of PS and PMMA with a lateral interface.

Analysis was performed using a line scan with a beam diameter of 100  $\mu\text{m}$ , laser energy of 1.0 mJ and a scan speed of 0.05 mm/s across the boundary between the polymers. For the EI-MS measurement, the selected ion monitoring (SIM) mode was applied, and characteristic  $m/z$  values were chosen that are most abundant when ablating PS or PMMA, respectively. The intensities for these  $m/z$  ratios were accumulated, resulting in the transient signals depicted in Fig. 7. No signal was

observed during the first 0.2 min until the start of the laser ablation when the signal for PS increased. The lateral interface between the two polymer types of the sample can be identified at 0.63 min of the measurement when the signal for PMMA rises sharply as the PS signal strongly decreases.

This example clearly shows the superiority of this technique over other conventional (bulk) polymer analysis techniques like Py-GC-MS or FTIR, which would only allow the distinction and characterization of the homogenous polymer sample without providing spatially resolved information. The collection of spatially resolved data is another special feature of the direct coupling of LA and EI-MS and is impossible with the approaches known from the literature. It provides the basis for depth profiling and imaging of samples.

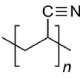
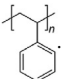

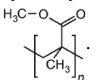
### 3.3. Classification and differentiation of polymers

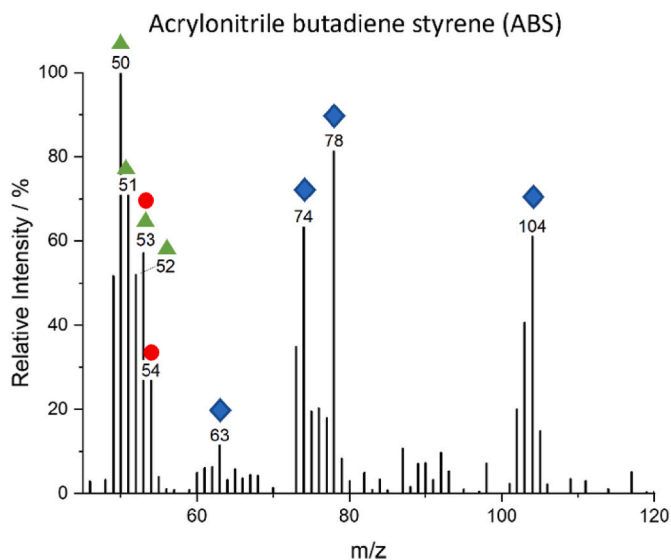
Three polystyrene samples from everyday life, namely a CD case, packaging material (Styrofoam) and a serving tray and one PMMA sample (a plastic microscope slide), were investigated using the optimized LA-EI-MS/ICP-OES procedure. To determine the ICP-OES signal intensities, the transient signals were integrated, background corrected, and normalized to the carbon signal.

For samples consisting of one specific polymer type with the same molecular structure, such as the three PS samples, the mass spectra were very similar and revealed only minor differences. The PMMA sample, on the contrary, had a different mass spectrum due to the different molecular structures of the polymer, allowing a clear distinction between the two types of samples.

Even though the polystyrene samples seemed identical in the EI-MS spectra, the distinction was possible using the elemental fingerprint obtained with the ICP-OES. The variations in the detected elements differed significantly, as indicated by the normalized signals presented in Fig. 8. To evaluate the achieved sensitivity, the LOD values for the

**Table 1**  
m/z values of detected fragments and tentative assignment of the elemental composition of these fragments.

m/z of fragment	Formula of fragment
<b>Polyacrylonitrile (PAN)</b>	
	
50	C <sub>3</sub> N
51	C <sub>3</sub> H <sub>N</sub>
52	C <sub>3</sub> H <sub>2</sub> N
53	C <sub>3</sub> H <sub>3</sub> N
<b>Polystyrene (PS)</b>	
	
51	C <sub>4</sub> H <sub>3</sub>
63	C <sub>5</sub> H <sub>3</sub>
74	C <sub>6</sub> H <sub>2</sub>
78	C <sub>6</sub> H <sub>6</sub>
91	C <sub>7</sub> H <sub>7</sub>
104	C <sub>8</sub> H <sub>8</sub>
<b>Polytetrafluoroethylene (PTFE)</b>	
	
50	CF <sub>2</sub>
69	CF <sub>3</sub>
81	C <sub>2</sub> F <sub>3</sub>
100	C <sub>2</sub> F <sub>4</sub>
<b>Poly(methyl methacrylate) (PMMA)</b>	
	
50	C <sub>4</sub> H <sub>2</sub>
69	C <sub>3</sub> HO <sub>2</sub>
100	C <sub>5</sub> H <sub>8</sub> O <sub>2</sub>



**Fig. 6.** LA-EI-MS spectrum of ABS showing the characteristic m/z fragments of the different monomers in the spectrum; m/z values of 50–53 are characteristic for acrylonitrile ( $\blacktriangle$ ), m/z of 53 and 54 show butadiene ( $\bullet$ ) and m/z of 63, 74, 78 and 104 originate from styrene ( $\blacklozenge$ ).

individual elements were calculated according to  $LOD = m_{Blank} + 3 \cdot s_{Blank}$ , where  $m_{Blank}$  is the mean value of the blank signal, and  $s_{Blank}$  is the associated standard deviation. The calculated LOD values were compared with the achieved signal values for individual elements of the

samples. Mg and Ca are both optimal for optical emission spectroscopy, with their signals being 400 and 45 times higher than the LOD values, respectively. For Ba, the signal corresponds to 5 times the LOD. Ti creates signals with a factor of 2 higher than that of the LOD, which still creates reliable qualitative results in the analysis. For the other monitored elements Al, Fe, Si and Sr, the ICP-OES signal shows no difference between the blank signal and the sample signal, hence these elements were assumed to not be present in the sample at detectable concentration levels.

In the case of the investigated polystyrene samples, the signals for the elements Ca, Mg, Ba and Ti showed significant alterations, enabling a simple differentiation of the three samples without advanced statistical methods.

Moreover, the sampling with laser ablation also enabled the differentiation between additives (being evenly distributed in the bulk material) and surface contaminants. For that purpose, the laser shots were arranged in a meander pattern with a scan speed of 0.6 mm/s to achieve a slight overlap of the laser shots with 100  $\mu$ m diameter and 10 Hz frequency. After the ablation process of the sample and analysis of the ablation products, the laser pattern was placed in the exact same position on the sample and fired again. Thus, during the first ablation, mainly sample material of the surface reached the detection units, while during the subsequent second ablation process, the material of the sample bulk was analyzed.

As shown in Fig. 8, for the serving tray sample, the normalized intensity for Calcium decreases significantly from the first to the second ablation process, indicating that more Calcium is on the surface than in the bulk material, thus showing Calcium contaminations on the surface. For Barium and Titanium, on the other hand, the normalized intensities are stable over the ablation processes indicating a homogenous distribution of the elements throughout regarding the sample surface and bulk. This homogeneity suggests that Ba and Ti are additives rather than contaminants. The EI-MS spectra detected concurrently showed no differences between the ablation processes, thus showing the homogeneity of the organic compositions when comparing the surface and bulk of the sample.

Likewise, for the CD case sample, enhanced normalized Ca intensities could be detected on the surface. Mg also appeared on the surface at higher levels than in the bulk of the material, meaning both Ca and Mg surface contamination could be detected. These contaminations on the surface most likely stem from touching the samples. For the Styrofoam sample, only a slight Ca contamination was determined. The bulk material of the microscope slide showed inorganic constituents very similar to the CD case. The elemental fingerprint only differed significantly regarding their surface contaminations. However, since the molecular structure of the samples differs, the concurrent EI-MS measurement allows the distinction with ease.

#### 4. Conclusions

When investigating composite polymer samples with conventional analytical methods, no concurrent molecular and elemental information of the samples is available, compromising the capabilities for complete sample characterization. In this work, it could be shown that laser ablation with parallel EI-MS/ICP-OES online detection can be a valuable new approach for advanced polymer characterization. A dedicated ablation cell was designed to directly connect the laser ablation process with EI-MS and ICP-OES to enable bimodal detection. Several parameters, including the carrier gas flow, the laser energy and the length and temperature of the transfer capillary, were carefully optimized to create the best possible measurement conditions.

The main advantages of the procedure are the concurrent measurement of molecular and elemental sample information and the possibility of performing spatially resolved investigations. The method allows advanced classification, discrimination and characterization of polymeric samples on the basis of both their organic and inorganic

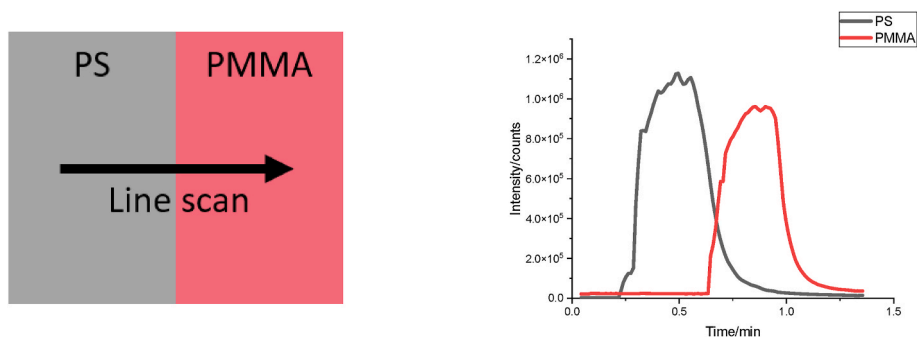


Fig. 7. Schematic setup of the PS-PMMA sample (left) and summed intensity for characteristic fragments for PS and PMMA showing the lateral resolution of a sample with a boundary between the two polymers (right).

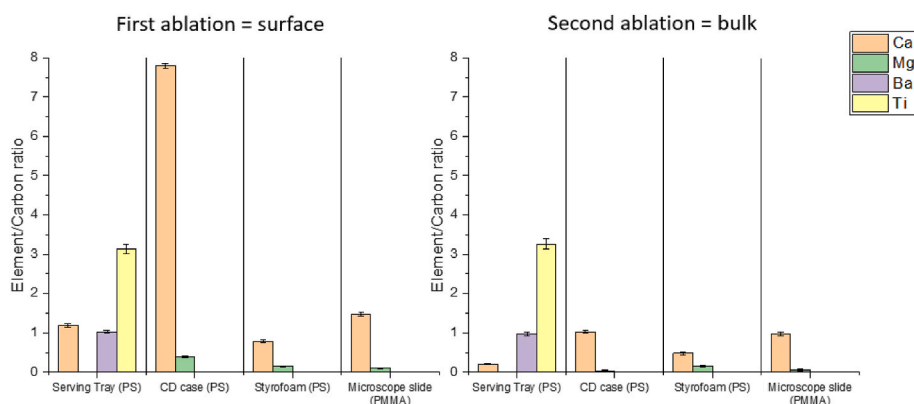


Fig. 8. Element-to-carbon ratio of three different polystyrene samples and the PMMA sample detected with ICP-OES of the two-layered consecutive ablation processes.

composition. Furthermore, it allows quick measurements with minimal to no sample preparation.

The proposed procedure has successfully been applied to the analysis of various polymer samples from everyday life, including three polystyrene samples from different uses. A distinction between the three polystyrene samples is only possible using the elemental data from the ICP-OES measurement. The developed approach furthermore allows the depth-resolved differentiation between surface and bulk information. Moreover, also laterally resolved measurement of the sample surface is possible.

Since the developed measurement setup also allows the coupling with ICP-MS, higher sensitivity for certain elements could be achieved. Consequently, elements with lower concentrations could also be assessed, facilitating the classification and differentiation of samples.

Ongoing work will investigate the possibility of realizing depth profile measurements vital for the study of layered samples. With the chemometric and statistical evaluation of data, more information about the constituents of the sample can be gained, which allows the differentiation of polymers with similar molecular structures and elemental fingerprints. Furthermore, the developed procedure can also be applied in the analysis of other solid samples made up of organic and inorganic constituents.

#### CRedit authorship contribution statement

**Laura Kronlachner:** Methodology, Investigation, Writing – original draft, Visualization. **Johannes Frank:** Methodology. **Erwin Rosenberg:** Conceptualization, Writing – review & editing. **Andreas Limbeck:** Conceptualization, Writing – review & editing, Supervision, Project administration, Resources, Funding acquisition.

#### Declaration of competing interest

The authors declare that they have no known competing financial interests or personal relationships that could have appeared to influence the work reported in this paper.

#### Data availability

Data will be made available on request.

#### Acknowledgments

The authors acknowledge TU Wien Bibliothek for financial support through its Open Access Funding Program.

#### References

- [1] M.P. Stevens, *Polymer Chemistry - an Introduction*, Oxford University Press, New York, 1999.
- [2] N.P. Cheremisinoff, *Polymer Characterization*, Noyes Publication, Westwood, NJ, 1996.
- [3] A.J. Peacock, A. Calhoun, *Polymer Chemistry - Properties and Applications*, Hanser Gardner Publications, Inc., Cincinnati, OH, 2012.
- [4] J.R.W.D. Campbell, R.A. Pethrick, *Polymer Characterization - Physical Techniques*, Taylor & Francis Group, Boca Raton, FL, 2000.
- [5] C. Moreta, M.T. Tena, Determination of plastic additives in packaging by liquid chromatography coupled to high resolution mass spectrometry, *J. Chromatogr. A* 1414 (2015) 77–87, <https://doi.org/10.1016/j.chroma.2015.08.030>.
- [6] F. Akoueson, et al., Identification and quantification of plastic additives using pyrolysis-GC/MS: a review, *Sci. Total Environ.* 773 (2021), <https://doi.org/10.1016/j.scitotenv.2021.145073>.
- [7] J. Vlachopoulos, D. Strutt, Polymer processing, *Mater. Sci. Technol.* 19 (9) (2003) 1161–1169, <https://doi.org/10.1179/026708303225004738>.
- [8] D.G. Baird, D.I. Collias, *Polymer Processing: Principles and Design*, John Wiley & Sons, Inc., Hoboken, NJ, 2014.
- [9] M.J. Bevis, *Recycling of Polymers*, Wiley-VCH, Weinheim, Germany, 1984.



- [10] R.S. Stein, Polymer recycling: opportunities and limitations, *Proc. Natl. Acad. Sci. U.S.A.* 89 (3) (1992) 835–838, <https://doi.org/10.1073/pnas.89.3.835>.
- [11] A. Dorigato, Recycling of polymer blends, *Adv. Ind. Eng. Polym. Res.* 4 (2) (2021) 53–69, <https://doi.org/10.1016/j.aiepr.2021.02.005>.
- [12] C. Burnier, G. Massonnet, Forensic analysis of condom traces: chemical considerations and review of the literature, *Forensic Sci. Int.* 310 (2020), <https://doi.org/10.1016/j.forsciint.2020.110255>.
- [13] J.V. Goodpaster, E.A. Liszewski, Forensic analysis of dyed textile fibers, *Anal. Bioanal. Chem.* 394 (8) (2009) 2009–2018, <https://doi.org/10.1007/s00216-009-2885-7>.
- [14] J. Zieba-Palus, G. Zadora, J.M. Milczarek, P. Kościelniak, Pyrolysis-gas chromatography/mass spectrometry analysis as a useful tool in forensic examination of automotive paint traces, *J. Chromatogr. A* 1179 (1) (2008) 41–46, <https://doi.org/10.1016/j.chroma.2007.09.044>.
- [15] S. Farah, K.R. Kunduru, T. Tsach, A. Bentolila, A.J. Domb, Forensic comparison of synthetic fibers, *Polym. Adv. Technol.* 26 (7) (2015) 785–796, <https://doi.org/10.1002/pat.3540>.
- [16] H. Pasch, Hyphenated techniques in liquid chromatography of polymers, *Adv. Polym. Sci.* 150 (2000) 2–66, [https://doi.org/10.1007/3-540-48764-6\\_1](https://doi.org/10.1007/3-540-48764-6_1).
- [17] E. Uliyanchenko, S. Van Der Wal, P.J. Schoenmakers, Challenges in polymer analysis by liquid chromatography, *Polym. Chem.* 3 (9) (2012) 2313–2335, <https://doi.org/10.1039/c2py20274c>.
- [18] V.G. Berezkin, I.B. Alishoyev, Viktor R. Nemirovskaya, *Gas Chromatography of Polymers*, Elsevier, Amsterdam, The Netherlands, 2011.
- [19] Y. Yampolskii, N. Belov, Investigation of polymers by inverse gas chromatography, *Macromolecules* 48 (19) (2015) 6751–6767, <https://doi.org/10.1021/acs.macromol.5b00895>.
- [20] A. Käßler, et al., Analysis of environmental microplastics by vibrational microspectroscopy: FTIR, Raman or both? *Anal. Bioanal. Chem.* 408 (29) (2016) 8377–8391, <https://doi.org/10.1007/s00216-016-9956-3>.
- [21] J.L. Xu, K.V. Thomas, Z. Luo, A.A. Gowen, FTIR and Raman imaging for microplastics analysis: state of the art, challenges and prospects, *TrAC, Trends Anal. Chem.* 119 (2019), 115629, <https://doi.org/10.1016/j.trac.2019.115629>.
- [22] J.M. Chalmers, N.J. Everall, Polymer analysis and characterization by FTIR, FTIR-microscopy, Raman spectroscopy and chemometrics, *Int. J. Polym. Anal. Char.* 5 (3) (1999) 223–245, <https://doi.org/10.1080/10236669908009739>.
- [23] G. Montaudo, F. Samperi, M.S. Montaudo, Characterization of synthetic polymers by MALDI-MS, *Prog. Polym. Sci.* 31 (3) (2006) 277–357, <https://doi.org/10.1016/j.progpolymsci.2005.12.001>.
- [24] M.W.F. Nielen, MALDI time-of-flight mass spectrometry of synthetic polymers, *Mass Spectrom. Rev.* 18 (5) (1999) 309–344, [https://doi.org/10.1002/\(SICI\)1098-2787\(1999\)18:5<309::AID-MAS2>3.0.CO;2-L](https://doi.org/10.1002/(SICI)1098-2787(1999)18:5<309::AID-MAS2>3.0.CO;2-L).
- [25] L. Li, *MALDI Mass for Synthetic Chemical Analysis*, John Wiley & Sons, Inc., Hoboken, NJ, 2010.
- [26] S. Tsuge, H. Ohtani, Structural characterization of polymeric materials by Pyrolysis-GC/MS, *Polym. Degrad. Stabil.* 58 (1–2) (1997) 109–130, [https://doi.org/10.1016/S0141-3910\(97\)00031-1](https://doi.org/10.1016/S0141-3910(97)00031-1).
- [27] R. Rial-Otero, M. Galesio, J.L. Capelo, J. Simal-Gándara, A review of synthetic polymer characterization by pyrolysis-GC-MS, *Chromatographia* 70 (3–4) (2009) 339–348, <https://doi.org/10.1365/s10337-009-1254-1>.
- [28] A. Gopanna, R.N. Mandapati, S.P. Thomas, K. Rajan, M. Chavali, Fourier transform infrared spectroscopy (FTIR), Raman spectroscopy and wide-angle X-ray scattering (WAXS) of polypropylene (PP)/cyclic olefin copolymer (COC) blends for qualitative and quantitative analysis, *Polym. Bull.* 76 (8) (2019) 4259–4274, <https://doi.org/10.1007/s00289-018-2599-0>.
- [29] A. Limbeck, P. Galler, M. Bonta, G. Bauer, W. Nischkauer, F. Vanhaecke, Recent Advances in Quantitative LA-ICP-MS Analysis: Challenges and Solutions in the Life Sciences and Environmental Chemistry, 2015, pp. 6593–6617, <https://doi.org/10.1007/s00216-015-8858-0>.
- [30] J.S. Becker, et al., Bioimaging of metals by laser ablation inductively coupled plasma mass spectrometry (LA-ICP-MS), *Mass Spectrom. Rev.* 29 (1) (2010) 156–175.
- [31] R. Srinivasan, B. Braren, Ultraviolet laser ablation of organic polymers, *Chem. Rev.* 89 (6) (1989) 1303–1316, <https://doi.org/10.1021/cr00096a003>.
- [32] Y. Choi, H. Lee, S.T. Fountain, D.M. Lubman, *Direct Chemical Analysis of UV Laser Ablation Products of Organic Polymers by Using Selective Ion Monitoring Mode in Gas Chromatography/Mass Spectrometry*, 1994.
- [33] P.F. Greenwood, S.C. George, M.A. Wilson, K.J. Hall, A new apparatus for laser micropyrolysis - gas chromatography/mass spectrometry, *J. Anal. Appl. Pyrolysis* 38 (1–2) (1996) 101–118, [https://doi.org/10.1016/S0165-2370\(96\)00948-5](https://doi.org/10.1016/S0165-2370(96)00948-5).
- [34] H. Watanabe, M. Yamamoto, Laser ablation of poly(ethylene terephthalate), *J. Appl. Polym. Sci.* 64 (6) (1997) 1203–1209, [https://doi.org/10.1002/\(SICI\)1097-4628\(19970509\)64:6<1203::AID-APP21>3.0.CO;2-V](https://doi.org/10.1002/(SICI)1097-4628(19970509)64:6<1203::AID-APP21>3.0.CO;2-V).
- [35] W. E. Wallace, “Mass spectra,” in *NIST Chemistry WebBook*, NIST Standard Reference Database Number 69, P. J. Linstrom and W. G. Mallard, Eds. Gaithersburg MD: National Institute of Standards and Technology.